Hartmann vs. reverse Hartmann test: a Fourier optics point of view

François Hénault, Cyril Pannetier

Institut de Planétologie et d'Astrophysique de Grenoble
Université Grenoble-Alpes
Centre National de la Recherche Scientifique
BP 53, 38041 Grenoble – France

Plan of presentation

- Principles of direct and reverse Hartmann tests
- Reverse Hartmann Wavefront Sensor (WFS)
  - Principle – Optical layout
  - Theoretical model and relations
  - Wavefront Error (WFE) slopes reconstruction
- Application to the Shack-Hartmann WFS
  - Similarities with reverse Hartmann WFS
  - Fourier optics model
- Numerical simulations
  - Input parameters and studied cases
  - Numerical results
- Conclusion

Direct and reverse Hartmann tests

A. **Direct Hartmann**: Set a grid of pinholes at the pupil plane of an aberrated optical system, and observe a distorted grid near (but not at) the image plane → **Modern Shack-Hartmann WFS**

B. **Reverse Hartmann**: Set the grid near (but not at) the image plane, and observe its distorted image at the pupil plane

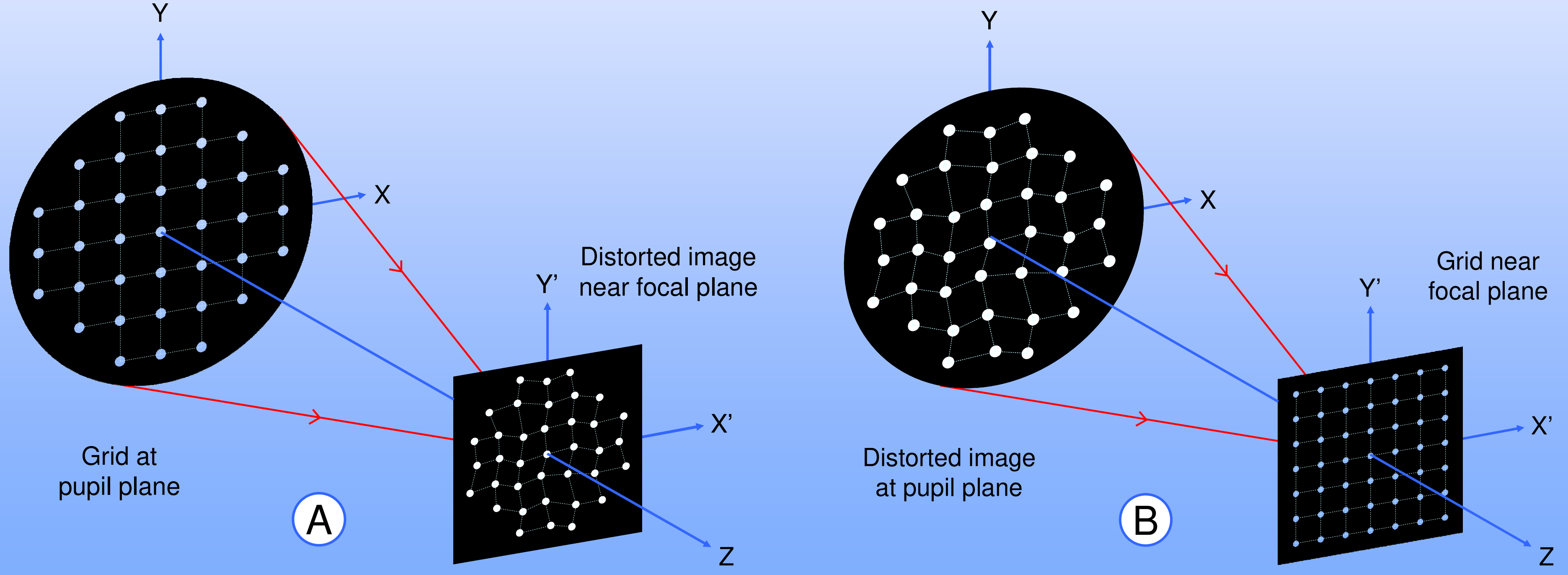

Reverse Hartmann Wavefront Sensor

- Principle – Optical layout

- This is a **pupil plane WFS**: a backward gazing camera forms an image of the pupil plane seen through a spatial filter
- The filter is located between the pupil and focal planes, at a distance *z'* from the camera
- Accurate WFE measurements are feasible when the period of the spatial filter and distance *z'* are optimized

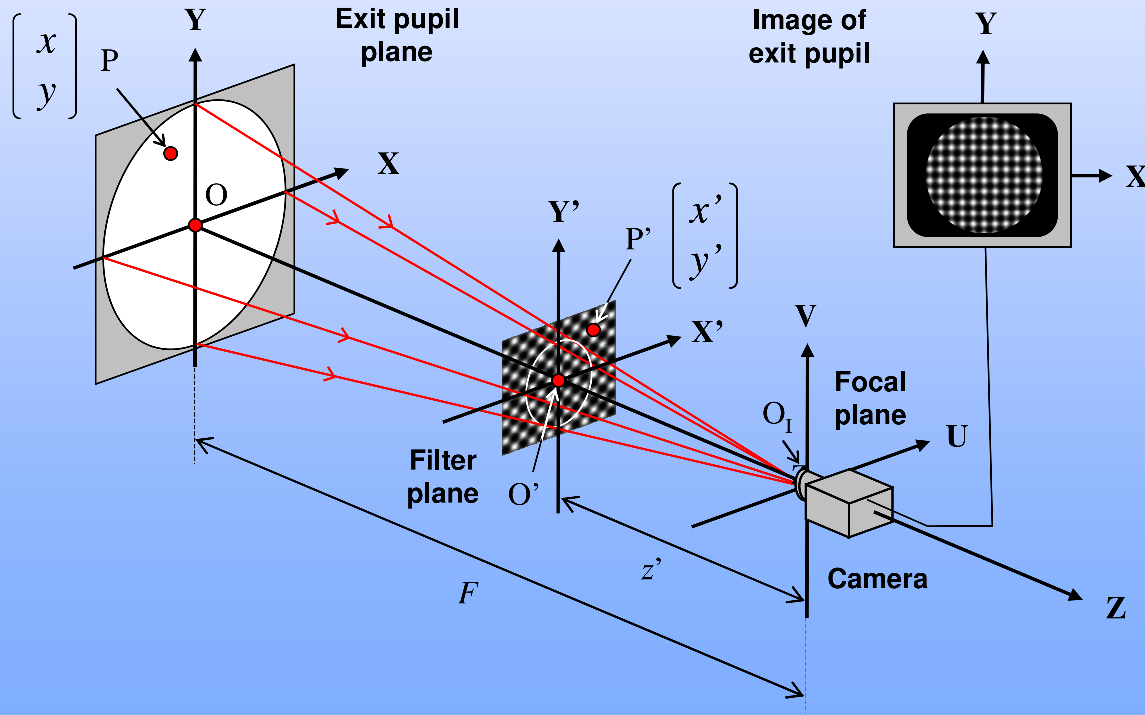

Reverse Hartmann Wavefront Sensor

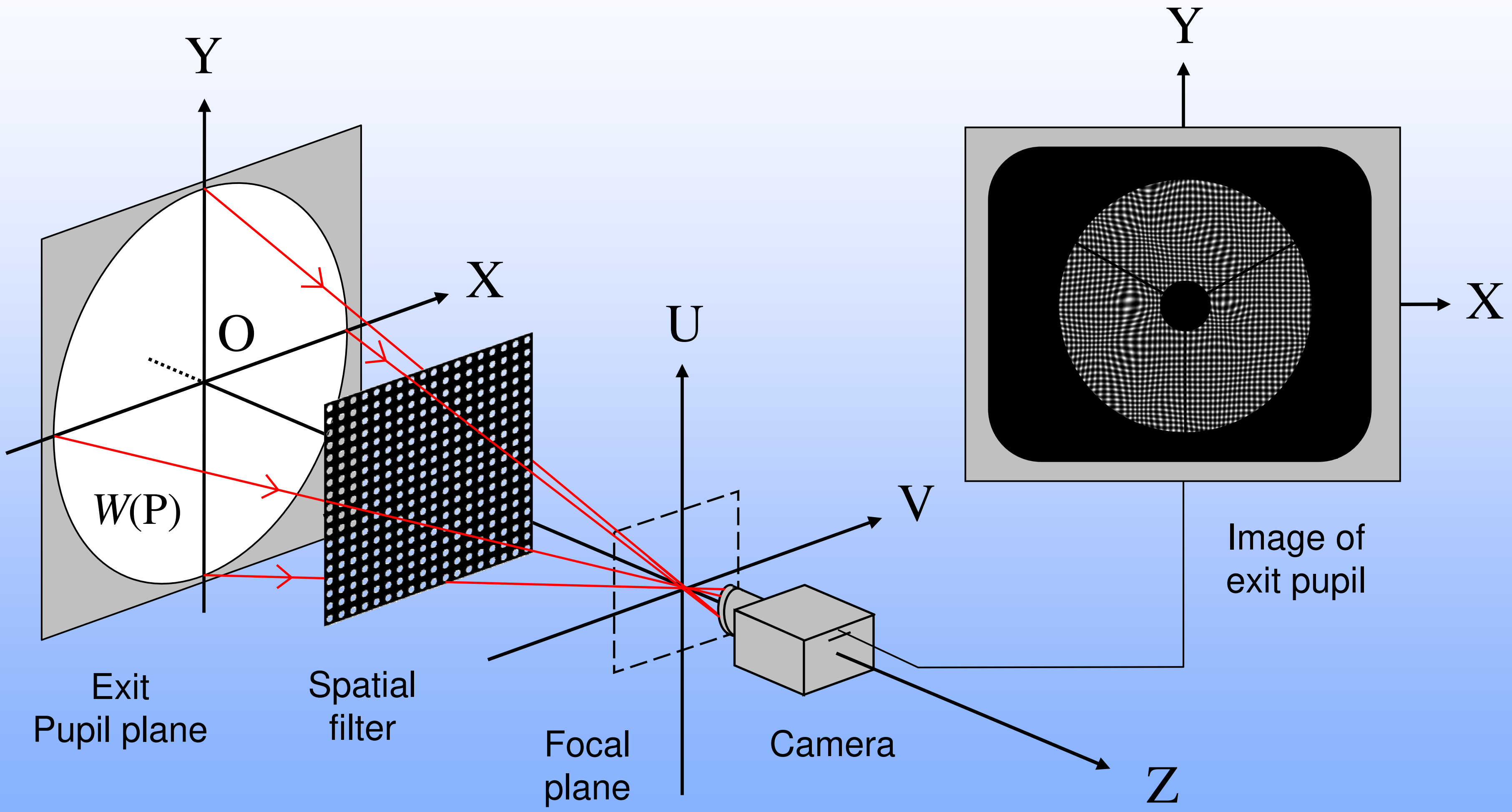

F. Hénault, JOSA A vol. 35, p. 1717-1729 (2018)

Reverse Hartmann Wavefront Sensor

- Two different types of spatial filters are usable

	Filter transmission $\mathrm{T}(x', y')$	Power spectrum $\left|FT[\mathrm{T}(x', y')]\right|^2$
Square Ronchi grating	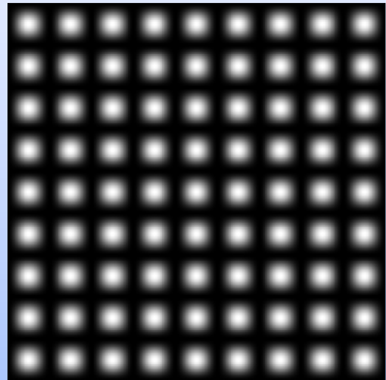	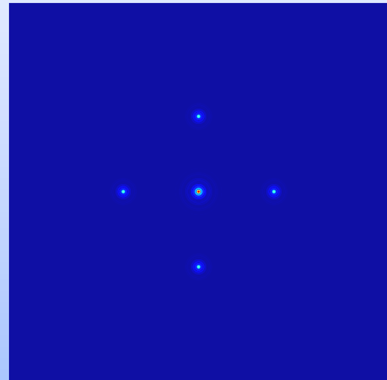
Hartmann grid (pinholes)	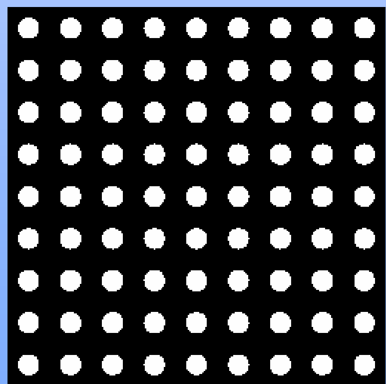	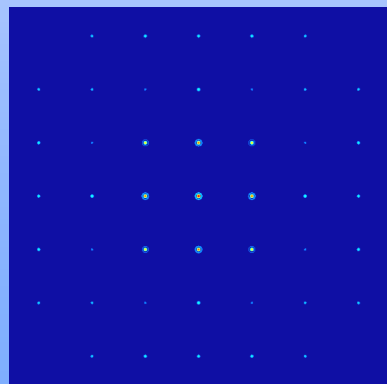

Reverse Hartmann Wavefront Sensor

- Theoretical model
  - Only Fresnel diffraction theory allows complete description of the instrument
  - The model can be simplified by retro-propagating complex amplitude from the filter to the pupil planes

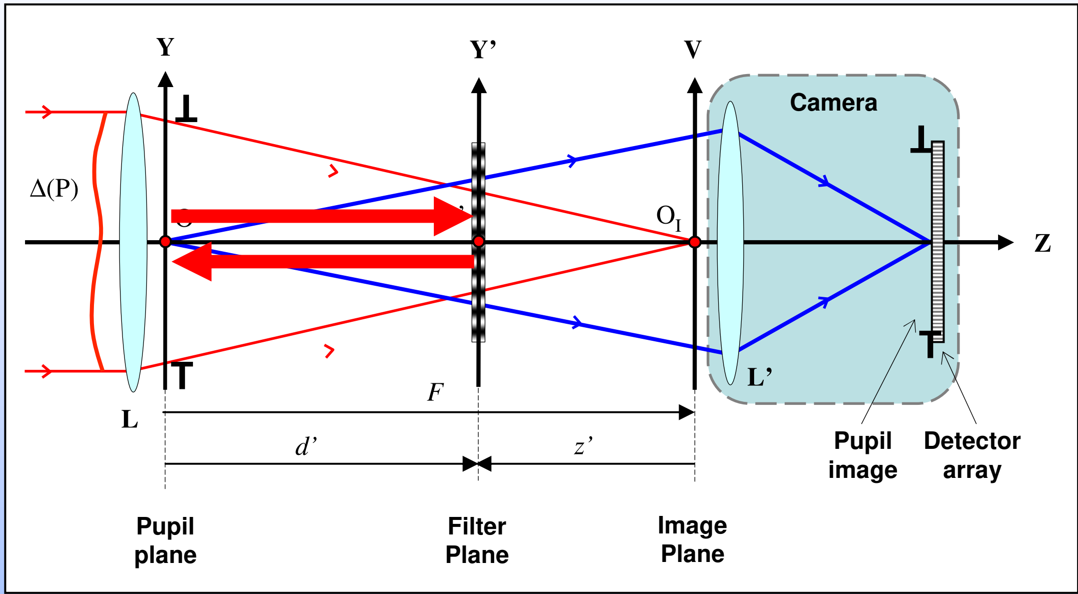

- Performance criteria:
  - Relative pupil shift $\rho = \lambda N\left(1 + z'/F\right)/p$
  - Lines number over pupil $n_M = |z'| f / N$
  - Gain $g = 2\pi\left(F + z'\right)/p$
  - Contrast $C(\lambda) = \cos\left[\pi\lambda z' F\left(1 + z'/F\right)/p^2\right]$

Spatial resolution

Signal-to-Noise Ratio

Wavefront error slopes reconstruction

- Spatial demodulation using a double Fourier transform algorithm
  - Start with the measured Hartmann-gram
  - Returns complex distributions whose phases are proportional to the slopes along X and Y axes

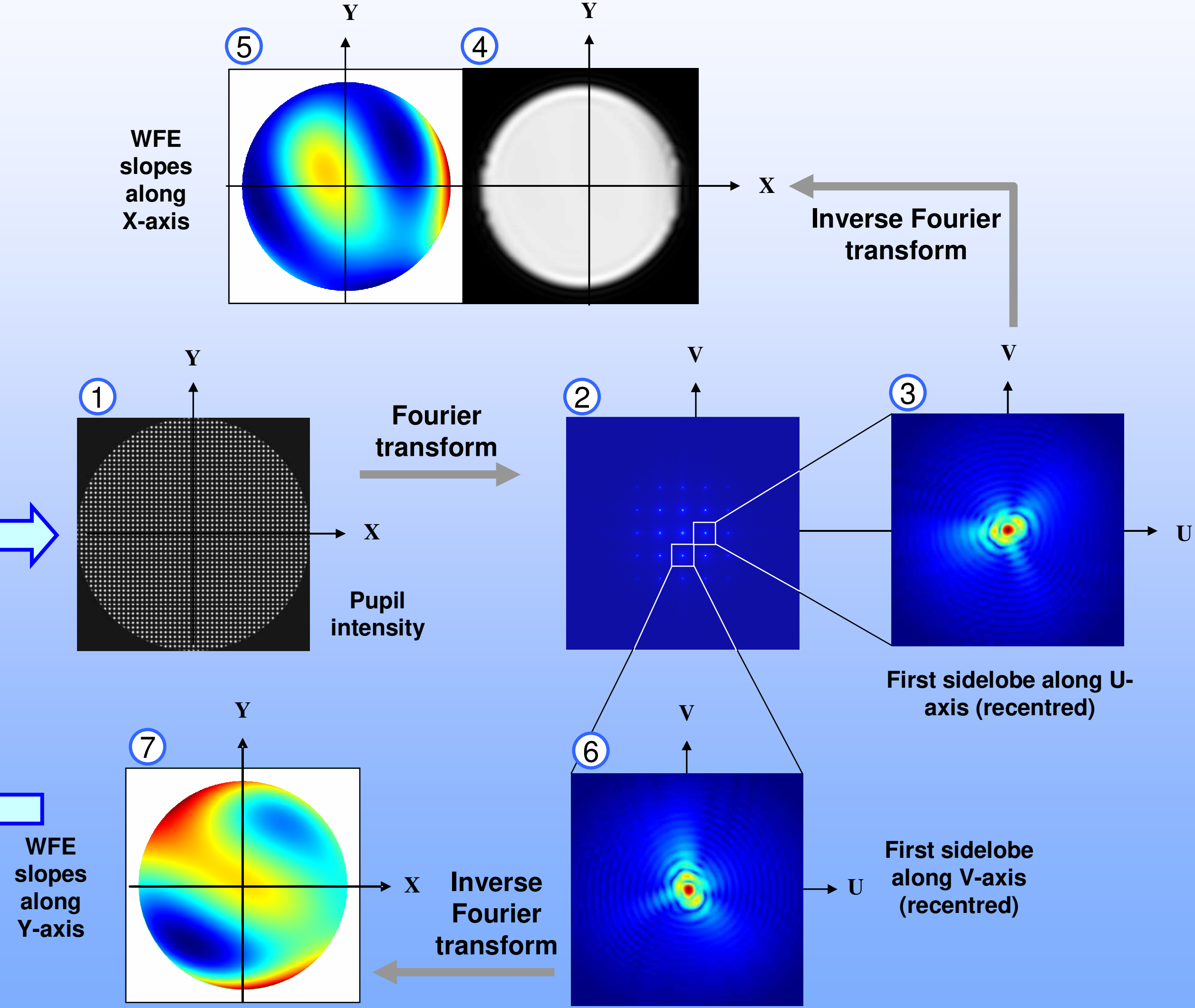

Application to the Shack-Hartmann WFS

- **Empirical statement**: Similar analytical relations govern the locations of the image spots for both WFS types:
  - Shack-Hartmann WFS (SH-WFS)

$$\boxed{\begin{aligned} x'_m &= m\,p - f\,\partial\Delta(x,y)/\partial x \\ y'_n &= n\,p - f\,\partial\Delta(x,y)/\partial y \end{aligned}}$$

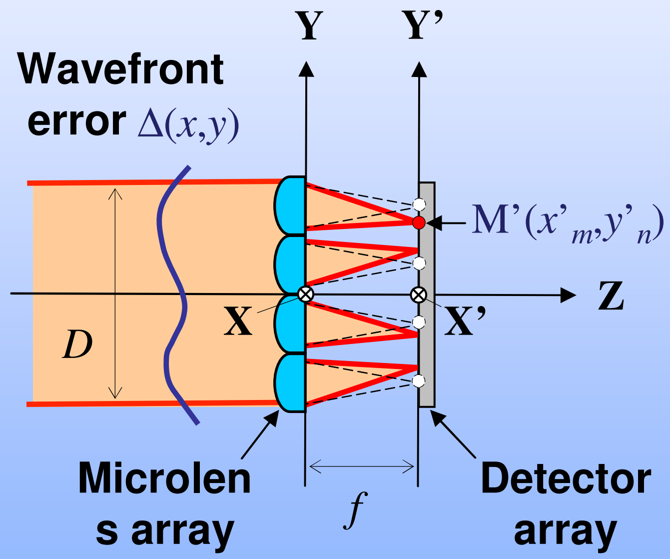

  - Reverse Hartmann WFS (RH-WFS)

$$\boxed{\begin{aligned} x_m &= m\,F\,p'/z' - d''\,\partial\Delta(x,y)/\partial x \\ y_n &= n\,F\,p'/z' - d''\,\partial\Delta(x,y)/\partial y \end{aligned}}$$

- Strong similarity suggests that RH-WFS image processing is also applicable to the SH-WFS → The **SH-IFT** method

Shack-Hartmann WFS optical model

- Pure Fourier optics model
  - A segmented array of linear phase ramps is added to the input wavefront
  - Recorded intensity on the SH-WFS detector array is computed as a Fraunhofer diffraction pattern
  - This model requires huge computing arrays (≥ 32767 x 32767)

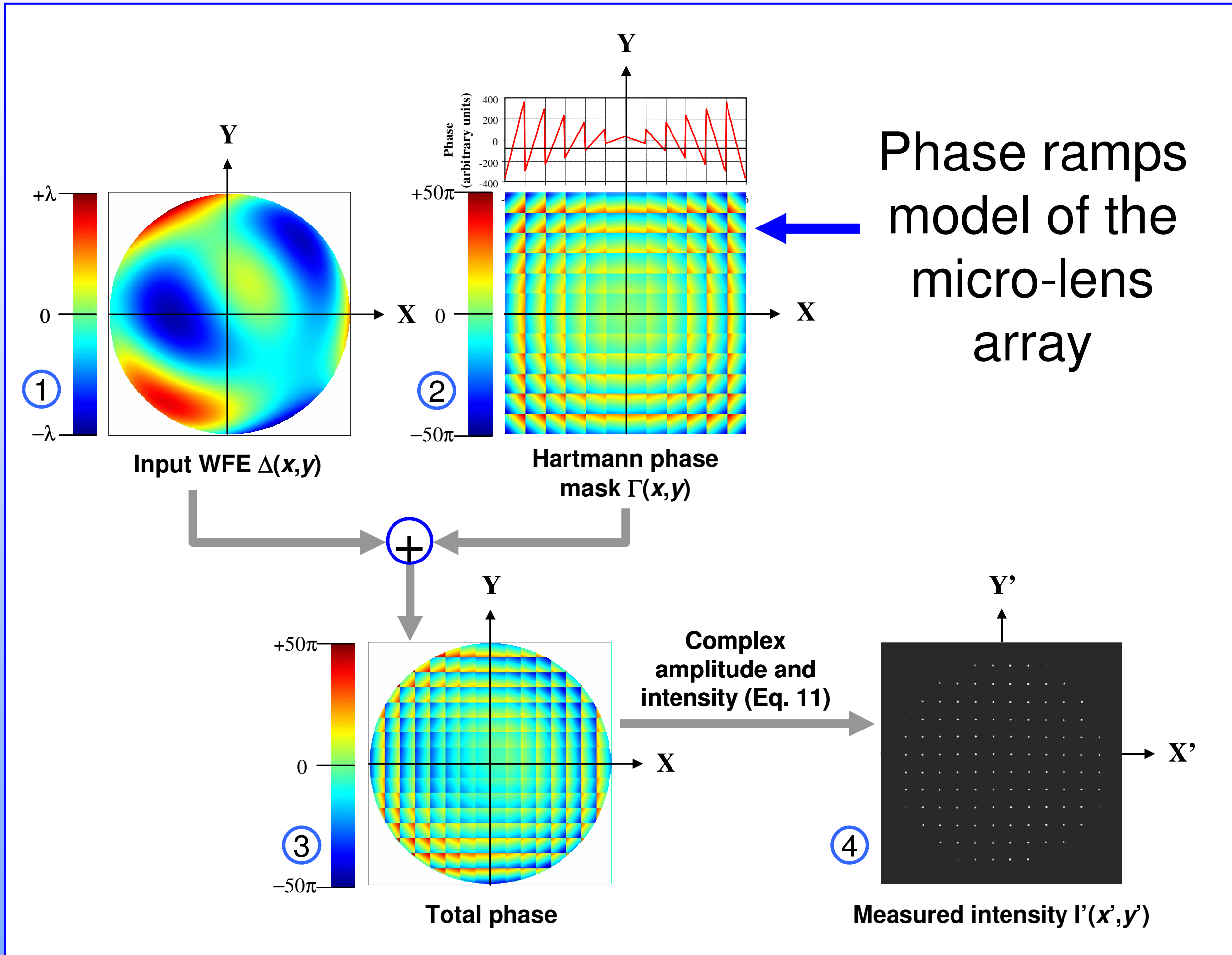

WFE slopes reconstruction – SH-IFT method

- Same reconstruction procedure as for the RH-WFS using a different gain factor
  - Raw intensity distributions recorded on the detector array
  - Output WFE slopes

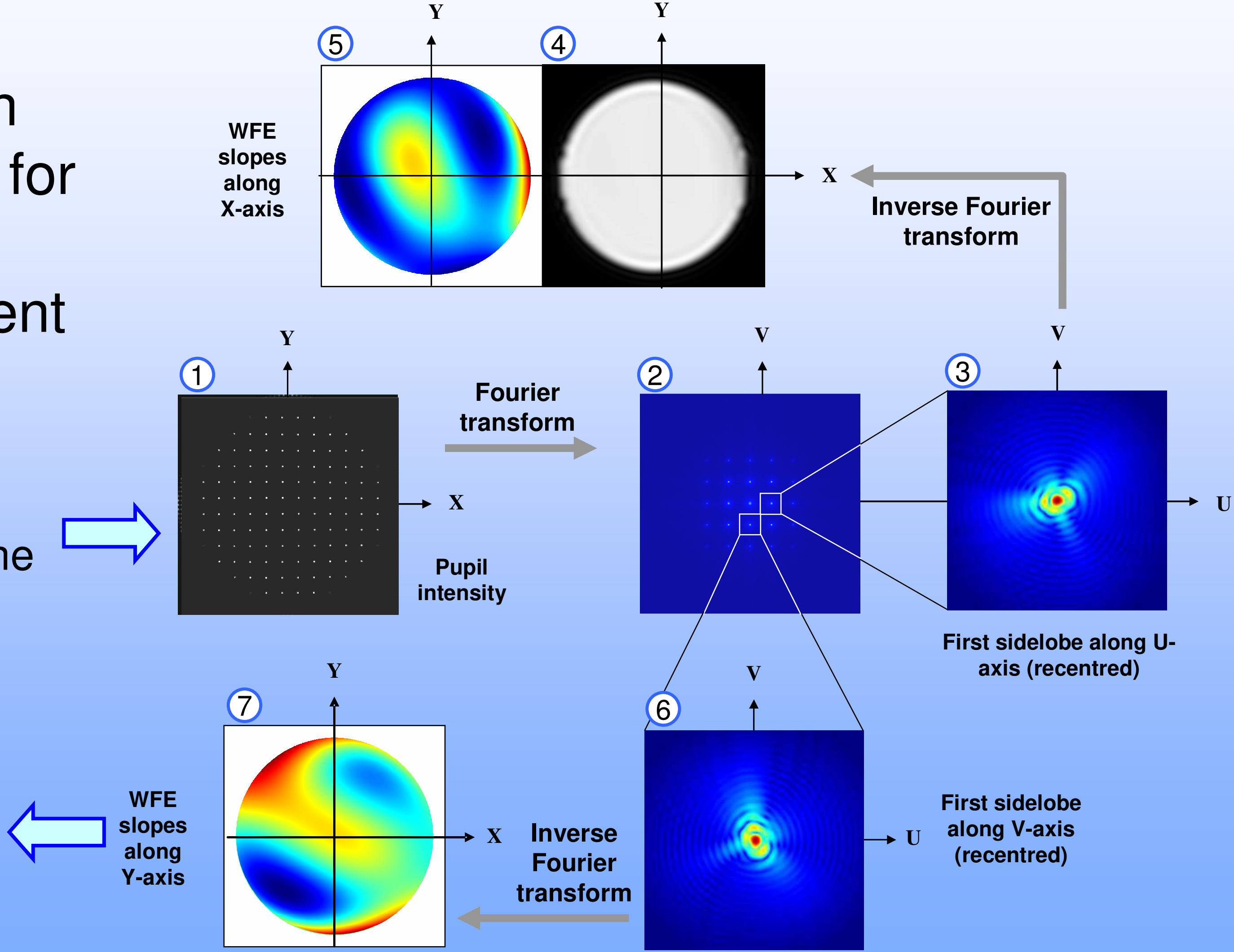

Numerical simulations (1/5)

- Input parameters and studied cases

- WFS type
  - RH-WFS vith square Ronchi grating
  - RH-WFS vith pinholes grid
  - SH-WFS using SH-IFT method

- Pupil sampling
  - 33 x 33
  - 65 x 65

Parameters	Symbol / Formula	*Pupil sampling* N x N		Unit
		33 x 33	65 x 65	
General / Tested optical system				
Reference wavelength	λ	0.6	0.6	µm
Focal length	F	1	1	m
Diameter	D	0.3	0.3	m
Aperture number	F/D	3.3	3.3	–
Square Ronchi / Reverse Hartmann test				
Image to filter distance	$z' = O_IO'$	-0.281	-0.490	m
Filter period	p'	2.64	2.30	mm
Relative pupil shear	See slide 6	0.05	0.04	%
Gain	See slide 6	1.7E+03	1.4E+03	–
Contrast (monochromatic)	See slide 6	0.999	0.996	–
Shack-Hartmann with SHIFT method				
Microlens array pitch / Microlens width	$p = D/N$	9.09	4.62	mm
Microlenses focal length	f	1000	1000	mm
Relative pupil shear	$\rho = \lambda f/pD$	0.022	0.043	%
Gain	$G = 2\pi f/p$	6.9E+02	1.4E+03	–

Numerical simulations (2/5)

- Reverse Hartmann WFS with square Ronchi grating

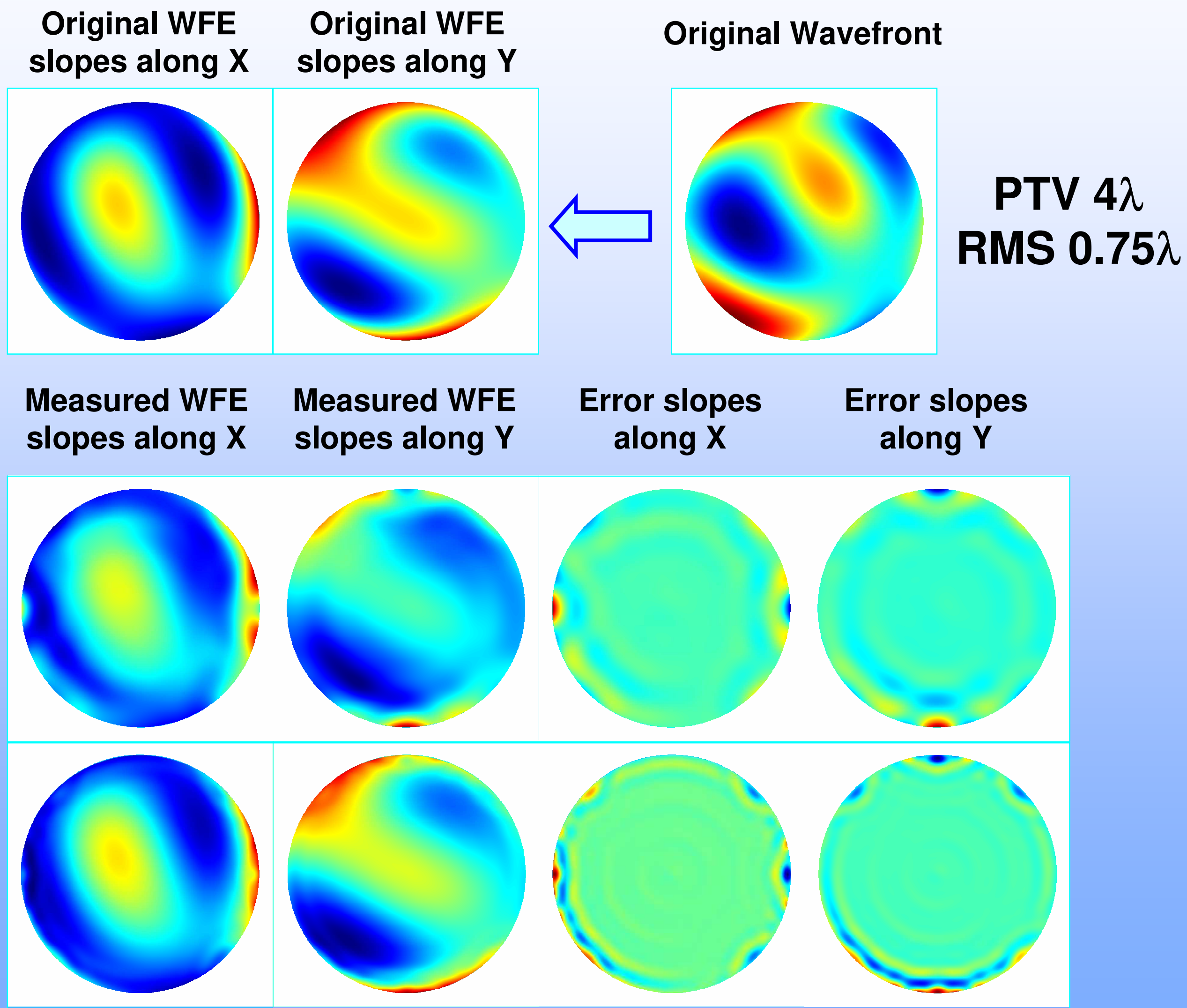

33 x 33
Measurement error
~ 25% RMS

65 x 65
Measurement error
< 10% RMS

Numerical simulations (3/5)

- Reverse Hartmann WFS with pinholes grid

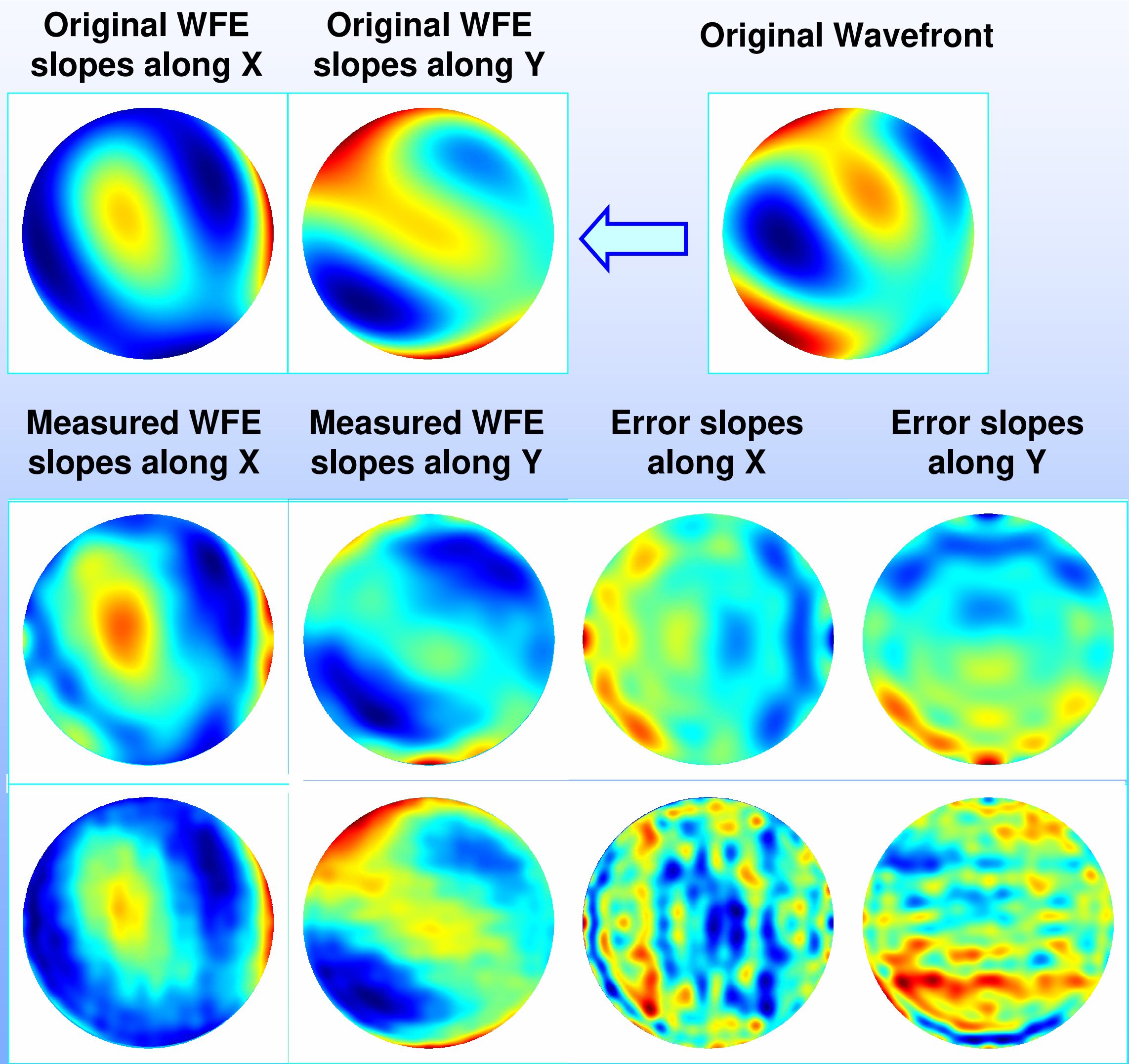

33 x 33
Measurement error
~ 50% RMS

65 x 65
Measurement error
< 20% RMS

Numerical simulations (4/5)

- Shack-Hartmann WFS using **SH-IFT** method

33 x 33

Measurement error

~ 15% RMS

65 x 65

Measurement error

< 10% RMS

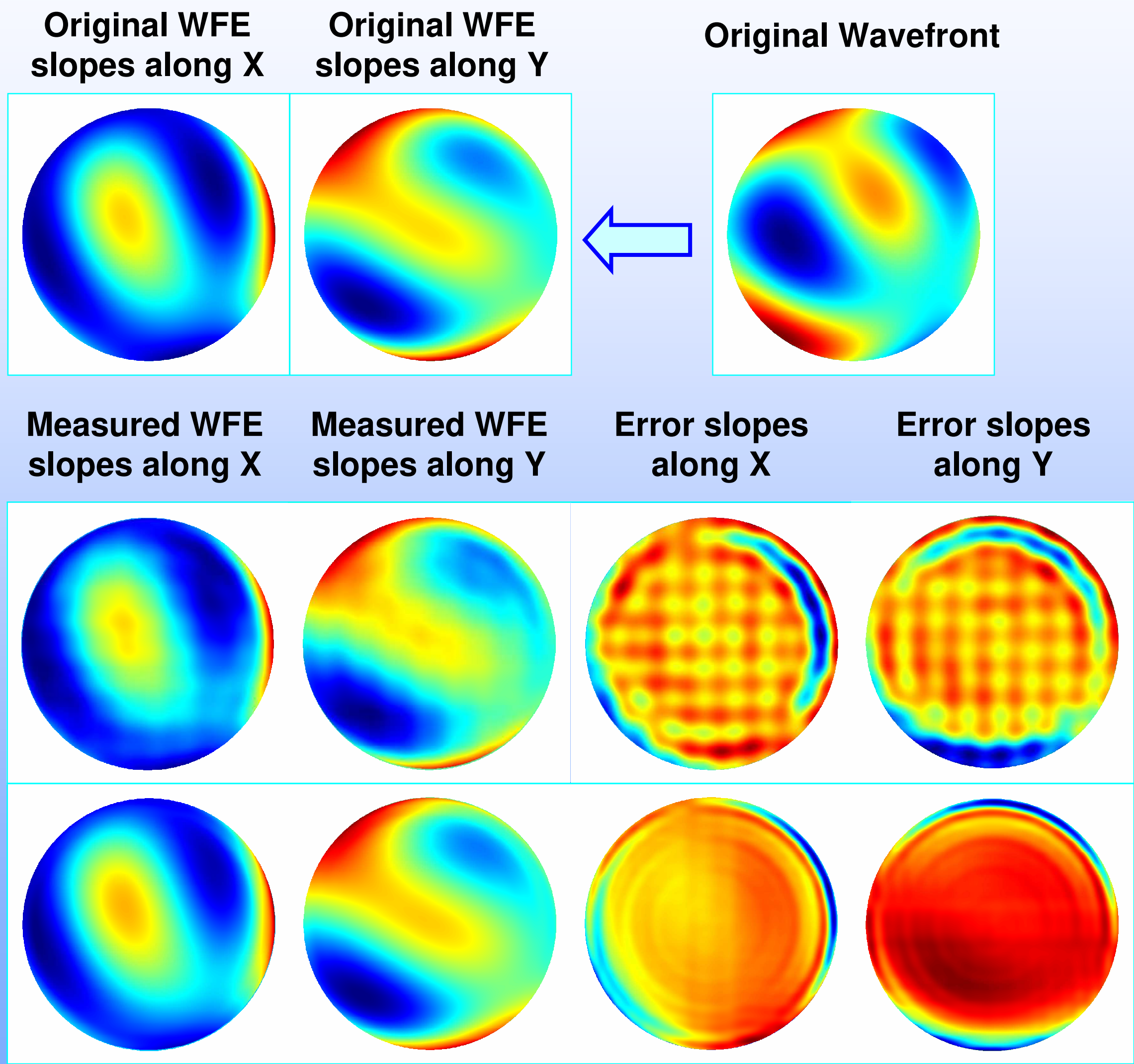

Numerical simulations (5/5)

- Best slopes measurement accuracy (**< 10% RMS**) is achieved by the RH-WFS equipped with a square Ronchi grating and by the SH-WFS using SH-IFT method
- Measurement accuracy improves with pupil sampling
- One may conclude that direct and reverse tests are equivalent

	Original WFE slopes	Measured slopes	Slopes difference	Relative error (%)	Original WFE slopes	Measured slopes	Slopes difference	Relative error (%)	
Square Ronchi test	Pupil sampling 33 x 33				Pupil sampling 65 x 65				
X-slopes (mrad)	0.052 0.010	0.070 0.010	0.059 0.003	114 26	0.052 0.010	0.057 0.010	0.017 0.001	32 9	PTV RMS
Y-slopes (mrad)	0.060 0.012	0.099 0.013	0.064 0.003	107 25	0.060 0.012	0.068 0.012	0.018 0.001	30 8	PTV RMS
SH-IFT method	Pupil sampling 33 x 33				Pupil sampling 65 x 65				
X-slopes (mrad)	0.051 0.010	0.054 0.010	0.009 0.001	17 13	0.051 0.010	0.052 0.010	0.006 0.001	12 8	PTV RMS
Y-slopes (mrad)	0.060 0.012	0.063 0.012	0.009 0.002	15 14	0.060 0.011	0.059 0.011	0.006 0.001	10 8	PTV RMS

Conclusion

- The historical Hartmann test is well-known and its principle gave birth to moderns Shack-Hartmann WFS
- The inverse Hartmann test is less known, but its principle can also be used in wavefront sensing for metrology, ophthalmology or astronomic applications
- Both types of wavefront sensors can be modeled using pure Fourier optics theory
- Numerical simulations show that they can achieve equivalent measurement accuracy if the reverse Hartmann WFS is equipped with a square Ronchi grating
- It is also found that the intensity distribution recorded by the SH detector array can be processed globally → The **SH-IFT** method

Thanks for your attention

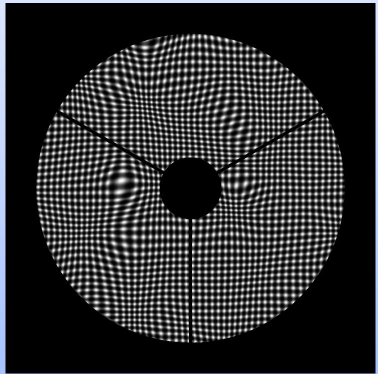

Questions ?